In vitro assembly and evaluation of Nora virus VLPs

Kellie D. Licking-Murray[#], Darby J. Carlson[#], Ryan Sowle, Kimberly A. Carlson[*]

Biology Department, University of Nebraska at Kearney, 2401 11th Avenue, Kearney, NE 68849, USA

Summary. – Nora virus is a RNA picorna-like virus that produces a persistent infection in *Drosophila melanogaster*. The genome is approximately 12,300 bases and is divided into four open reading frames (ORFs). Structurally, there are four important viral proteins: VP3, VP4A, VP4B, and VP4C. Three proteins (VP4A, VP4B, and VP4C) that form the virion's capsid are encoded by *ORF 4*, which produces a polyprotein that is post-translationally cleaved. The fourth protein (VP3) is encoded by *ORF 3* and it is hypothesized to play a role in virion stability. The genes for these proteins were individually cloned into *Escherichia coli*, expressed, and the proteins were purified. Virus-like particles (VLPs) were assembled *in vitro* by mixing the proteins together in different combinations and measured via electron microscopy. Assemblies that contained VP4A and/or VP3 created VLPs with similar sizes to purified empty Nora virus capsids, potentially indicating that VP4A and/or VP3 are vital for Nora virus capsid structure, assembly, and/or stability. Not only does this study provide insight into the role of Nora virus proteins, but it may also lead to a deeper understanding of how Nora virus or other picorna-like viruses undergo assembly.

Keywords: RNA viruses; Nora virus; picorna-like virus; virus-like particles; capsid assembly

Introduction

Nora virus is an isometric, non-enveloped, picorna-like virus that has a positive-sense, single stranded RNA (ssRNA) genome comprised of four ORFs (Habayeb *et al.*, 2006), which when combined, yield a size of approximately 12.3 kb (Ekström *et al.*, 2011). Being a picorna-like virus, it has three common characteristics of the superfamily: encoding of a type I RNA-dependent RNA polymerase (RdRp), the same coding region order for the replication module (helicase-protease-RdRp), and the production of large polyproteins. Even though picorna-like viruses share certain characteristics, there is abundant biodiversity from one another, such as viral shape, structure of the genome (one vs. two RNA segments), genome size, and location of capsid protein sequences in the genome (Sanfaçon,

2011). As expected, Nora virus has diversified from other picorna-like viruses by having differences that include a large genome consisting of four ORFs and the production of small RNAs, in addition to the large RNAs that result in polyproteins (Habayeb *et al.*, 2006). Also, Nora virus capsid protein sequences are not similar to other picorna-like viruses, while the sequences that encode the replication enzymes are most closely related to viruses from the families *Picornaviridae* and *Iflaviridae* (Habayeb *et al.*, 2006; Koonin *et al.*, 2008). As previously described, Nora virus shares common properties of picorna-like viruses but also differ in some aspects, which suggests that they belong in to a new family (Habayeb *et al.*, 2006) within the order *Picornavirales.*

Nora virus causes a persistent infection in *D. melanogaster* and is transmitted via the fecal-oral route (Habayeb *et al.*, 2009a,b). It is postulated that there are no known detrimental effects to *D. melanogaster* when retaining this virus, but a defect in geotaxis has recently been found (Rogers *et al.*, 2020). Some human *Picornaviridae* viruses, like poliovirus and coxsackievirus, are able to cause persistent infections that eventually lead to severe

*Corresponding author. E-mail: carlsonka1@unk.edu; phone: +308-865-1554. #Authors contributed equally.

health complications (Klingel *et al.* 1992; Rueckert, 1996). Therefore, using Nora viruses and *D. melanogaster* to study persistent infections could lead to insight involving other closely related human picornaviruses.

The four ORFs of Nora virus encode different types of proteins that have distinct functions. *ORF 1* encodes one protein, approximately 475 amino acids in length, which acts as a RNA interference (RNAi) suppressor (van Mierlo *et al.*, 2012). The product of *ORF 2* is approximately 2,100 amino acids and its sequence suggests it codes for the helicase-protease-replicase (H-P-Rep) cassette (Habayeb *et al.*, 2006). *ORF 3* encodes a 281–304 amino acid product (VP3), making this the shortest protein of Nora virus. The 281–304 amino acid range is due to a 71 nucleotide overlap of *ORF 3* with the C-terminus of *ORF 2,* and translation of *ORF 3* likely occurs from a frame shift mechanism (Ekström *et al.*, 2011). The VP3 protein is associated with the capsid and is suggested to provide stability to the virion structure (Ekström *et al.*, 2011, Sadanandan *et al.*, 2016). *ORF 4* encodes approximately 931 amino acids and consists of a polyprotein, which is cleaved proteolytically to make the major structural proteins (Ekström *et al.*, 2011). These viral proteins are VP4A (37 kDa), VP4B (32 kDa), and VP4C (49 kDa) (Ericson *et al.*, 2016). Even though VP3, VP4A, VP4B, and VP4C are components of the virus, there is little known as to how the capsid assembles and the importance played by these proteins in viral structure and/or stability. A main focus of this study was to determine these roles via the *in vitro* production of VLPs of Nora virus, which could lead to a deeper understanding of the Nora virus life cycle.

Studies of *in vitro* whole virus assembly date back to 1955 with the production of tobacco mosaic virus (Fraenkel-Conrat and Williams, 1955) and to 1967 for the first icosahedral virus, cowpea chlorotic mottle virus (Bancroft and Hiebert, 1967). Assembly of a complete virion is driven by two types of interactions: capsid protein-capsid protein and capsid protein-nucleic acid (Garmann *et al.*, 2014). By the early 1980s, viral assembly work advanced to the production of VLPs with over 100 successfully constructed and characterized VLPs for various viruses (Zeltins, 2012). VLPs are non-infectious since they lack the core genetic material and only contain the outer capsid protein shell (Grgacic and Anderson, 2006). They can form through spontaneous self-assembly of the capsid proteins (Pattenden *et al.*, 2005; Grgacic and Anderson, 2006; Sanchez-Rodriguez *et al.*, 2012) due to the interactions between neighboring protein molecules (capsid protein-capsid protein) forming the capsid (Garmann *et al.*, 2014).

Initially, VLPs were produced to study viral proteins and their role in virus assembly, stability, morphology, and replication (Carreira *et al.*, 2004). An example is work to determine the different protein combinations that could be assembled to form rotavirus-like particles. The particles formed provide information about the properties of rotavirus protein and particle structure, function, and assembly. Some proteins were found to be unnecessary for capsid assembly and others resulted in particles with a morphology similar to native rotavirus (Crawford *et al.*, 1994). In addition to rotavirus, other studies that looked at viral assembly using VLPs involved human immunodeficiency virus, hepatitis B virus, and influenza A virus (Noad and Roy, 2003). VLPs also have been used in vaccine production since they provide a safe template with favorable economics and can induce both innate and adaptive immune responses (Mohsen *et al.*, 2017). For this role, particles have been made against several viruses including enterovirus 71 (Chung *et al.*, 2008), coxsackievirus B3 (Zhang *et al.*, 2012), poliovirus (Bräutigam *et al.*, 1993), hepatitis B virus (Noad and Roy, 2003), and human papillomavirus (Koutsky *et al.*, 2002). Therefore, assembly of Nora virus VLPs is plausible.

Past research shows Nora virus to have an icosahedral capsid (T=1) composed of 3 proteins, VP4A, VP4B, and VP4C (Laurinmäki *et al.*, 2020) and VP3 having a role in capsid stability but not capsid formation (Sadanandan *et al.*, 2016). Laurinmäki *et al.* (2020) recently provided information on how these proteins interact and the roles they play in the capsid structure. N-termini interactions of VP4C and VP4B show a role in intra-pentamer stability while VP4A interacts with viral RNA and provides inter-pentamer stability. In this current study, the formation of VLPs by combining the different structural proteins *in vitro* was of interest to determine which proteins of Nora virus are essential in assembling the capsid. In addition to successfully producing VLPs to Nora virus and providing evidence for the structural capsid proteins, we aimed to identify if one of the viral proteins is acting as the major protein responsible for capsid formation and/or stability.

Materials and Methods

Cloning of Nora virus genes and protein purification. Nora virus genes, *ORF 3*, *ORF 4A*, *ORF 4B*, and *ORF 4C*, were cloned into *E. coli*, expressed, and the proteins were purified via affinity chromatography. To maximize expression, the genes were synthesized for codon and secondary structure optimization (GeneScript, USA) with the addition of a 6-histidine (his) tag at the C-terminus of each gene. Next, the genes were cloned into the *pET28a* vector (Novagen, USA) using the InFusion HD cloning kit (Clontech, USA). Transformed cells for the genes of interest were confirmed via PCR and restriction enzyme digestion. Positive plasmid DNA cloned inserts were used for transformation into One Shot® BL21 (DE3) pLysS chemically competent *E. coli* cells (Invitrogen, USA) in preparation for gene

expression. Overnight cultures of cells were subcultured and incubated at 37°C until mid-exponential phase (Abs_{600} = 0.5), when isopropylthio-β-galactoside (IPTG) was added to a final concentration of 1.0 mM and then allowed to incubate for an additional 24 h. The overnight culture of cells was harvested and prepared for immobilized metal affinity chromatography (IMAC) by centrifugation at 8,000 x *g* for 10 min at 4°C. Supernatants were removed and 10 volumes of lysis/wash buffer (300 mM KCl, 50 mM KH_2PO_4, pH 8.0, 20 mM Imidazole, 6 M Urea) were added to resuspend the pellets. Lysates were sonicated on ice for 15 s on and 15 s off pulses, for four minutes. Lysates were centrifuged at 12,000 x g for 10 min at 4°C. Supernatants were removed and microfiltered through a sterile 0.22 μm membrane (Thermo Fisher Scientific, USA). Purification of his-tagged proteins was done individually through separate 1.0 ml IMAC cartridges under denaturing conditions. A column packed with Profinity™ IMAC (BioRad, USA) resin was equilibrated with 5 column volumes of lysis/wash buffer at 2 ml/min. Sample lysates were loaded and run at a flow rate of 2 ml/min. The cartridge was washed with 6 column volumes of lysis/wash buffer at 2 ml/min followed by wash with 6 column volumes of wash buffer 2 (20 mM Tris, pH 8.0, 50 mM KCl, 20 mM Imidazole, 2 M Urea) at 2 ml/min. Proteins were eluted with 10 column volumes of elution buffer (20 mM Tris, pH 8.0, 50 mM KCl, 10 mM–250 mM Imidazole, 2 M Urea) at 2 ml/min, collected in 1.0 ml fractions, and analyzed by SDS-PAGE with Coomassie blue staining. Concentration of proteins was performed in triplicate using the Pierce™ BCA protein assay kit (Thermo Fisher Scientific) following manufacturer's instruction's.

In vitro assembly of VLPs. Capsid assembly was carried out by dialyzing 3.0 ml (50μg/ml) of recombinant protein (in different combinations) in a Slide-A-Lyzer cassette (Pierce, USA) against 500 ml of buffer 1 (20 mM Tris-HCl, pH 8, 150 mM NaCl, 5 mM $MgCl_2$, 5 mM $CaCl_2$, 0.3% Sarkosyl, 1 mM DTT, 1.5 M Urea) for one hour. The sample was removed from buffer 1 and placed against 500 ml of buffer 2 (20 mM Tris-HCl, pH 8, 150 mM NaCl, 5 mM $MgCl_2$, 5 mM $CaCl_2$, 0.3% Sarkosyl, 1 mM DTT, 1.0 M Urea) for one hour. It was removed and placed in 500 ml of buffer 3 (20 mM Tris-HCl, pH 8, 150 mM NaCl, 5 mM $MgCl_2$, 5 mM $CaCl_2$, 0.3% Sarkosyl, 1 mM DTT, 0.5 M Urea) for one hour, after which it was placed in 500 ml of buffer 4 (20 mM Tris-HCl, pH 8, 150 mM NaCl, 5 mM $MgCl_2$, 5 mM $CaCl_2$, 0.3% Sarkosyl, 1 mM DTT) for one hour. All assemblies were carried out at room temperature. The different combinations of proteins for VLP assembly include: VP3/4A/4B/4C, VP3/4B/4C, VP3/4A/4B, VP4A/4B/4C, VP3/4A, VP3/4B, VP3/4C, VP4A/4C, VP4B/4C, and VP4A.

To verify that the assembly of Nora virus VLPs was occurring without the influence of other factors, an IgG control was run. The control was set up by dialyzing 50 μg of IgG against 500 ml of buffer 3 (20 mM Tris-HCl, pH 8, 150 mM NaCl, 5 mM $MgCl_2$, 5 mM $CaCl_2$, 0.3% Sarkosyl, 1 mM DTT, 0.5 M Urea) for one hour and placed in a sucrose gradient layered with 1.0 ml of each 20% (10.0g), 15% (7.5g), 10% (5g), and 5% (2.5g) sucrose, from bottom

to top. Ultracentrifugation was performed in a Beckman L-60 Ultracentrifuge using an SW55 rotor at 28,000 x *g* for 2.0 h at 4°C. Protein in the gradient was recovered by gradient fractionation into ~0.5 ml fractions and analyzed via Western blotting using only secondary antibody, goat anti-mouse IgG Fc alkaline phosphatase conjugate (1:5,000 dilution, Pierce).

Collection of VLPs from assemblies. Samples were removed from the Slide-A-Lyzer cassettes and separated in cesium chloride (CsCl) gradients (2.0 ml of 1.5g/ml CsCl with 2.0 ml of 1.22 g/ml CsCl) with protease inhibitor cocktails (200 μl/CsCl layer, Simga-Aldrich, USA) added. Ultracentrifugation was performed in a Beckman L-60 Ultracentrifuge using an SW55 rotor at 28,000 x *g* for ~24 h at 4°C. Samples were recovered by gradient fractionation into ~0.5 ml fractions and analyzed via Western blotting for proteins from the assembly. Fractions containing Nora virus proteins were analyzed by electron microscopy (EM) to determine the presence or absence of assembled VLPs.

Western blot analysis of assembly fractions. Samples recovered from the gradient were separated by Mini-PROTEAN® TGX™ gels (BioRad) and transferred via the Trans-Blot® Turbo™ Transfer System (BioRad) to a Trans-Blot® Turbo™ 7.5% PVDF 0.2 μm nitrocellulose membrane (BioRad). Overnight blocking was performed on the membranes in 5% non-fat dry milk/ Tris-buffered saline + Tween 20 (TBST) at 4°C. The milk/TBST mixture was removed and fresh 5% non-fat dry milk/TBST with primary antibody (anti-Nora virus, 1:500 dilution) was added for 3 hours and incubated at room temperature. Preparation of the primary antibody was described in Ericson *et al.*, 2016. Detection was achieved with the secondary antibody, goat anti-mouse IgG Fc alkaline phosphatase conjugate (1:5,000 dilution, Pierce) and developed with NBT/BCIP (Pierce).

EM of assembly fractions. Samples were sent to the Electron microscopy core facility at the University of Nebraska Medical Center. Grids used for EM were 200 mesh copper grids coated with formvar and silicon monoxide (Ted Pella, Inc., USA). A 10 μl drop of each sample (from a positive Western blot result) was placed on the grid for one minute. The excess was wicked off with a piece of Whatman 50 filter paper and the grid was allowed to air dry for two minutes. A droplet of Nano-Van solution (Nanoprobes, Inc., USA) was placed on the grid for one minute. The excess was wicked off and the grid was allowed to dry for two minutes. The grids were examined in a Tecnai G2 Transmission Electron Microscope operated at 80Kv. Grids with VLPs had random particles selected and the diameters (in nm) were measured.

Data analysis. Electron microscopy measurement data were analyzed using a one-way ANOVA with a post-hoc Holm-Bonferroni test (Aickin and Gensler, 1996) comparing all VLP assembly protein combinations to the upper band (positive control) or VP4A (negative control, only one protein in the assembly) with significance prescribed as $p \leq 0.05$. In a previous study, a Nora virus purification was placed on a cesium chloride density gradient and the sample separated into two bands, re-

Results

VLPs assembly and fractions analysis by Western blot

A total of 50 µg per protein were added to each cassette for assembly of VLPs and several combinations of proteins were set-up. After assembly, each sample was placed in a CsCl gradient and fractions were collected in ~0.50 ml aliquots. To start the detection process of positive or negative VLP assembly, Western blot analysis was completed on the fractions and probed with anti-whole Nora virus antisera (1:500 dilution). Any fractions that had Nora virus protein detected were used for EM analysis. Two representative Western blots of VP3/4A/4B, and VP4B/4C assembly fractions are shown (Fig. 1) to represent Nora virus protein products VP3 (~35 kDa), VP4A (~37 kDa), VP4B (~32 kDa), and VP4C (~49 kDa).

VLPs measurement via electron microscopy

For confirmation of VLP assembly, fractions that contained products visualized via Western blot with the appropriate protein sizes were analyzed by EM. Diameters of VLPs were randomly taken from EM images by the core facility and the average particle diameter was calculated (Table 1). Representative EM images for VLPs from assemblies for VP3/4A and VP3/4A/4B/4C are shown in Fig. 2. Representative size distribution profiles for the particles from the Nora virus empty capsid upper band (control), VP3/4A, and VP3/4A/4B/4C are shown in Fig. 3.

Statistical analysis of different protein combinations producing VLPs

The upper band positive control was used to assess if formed VLPs from the various protein combinations

Fig. 1

Western blot analysis of CsCl gradient fractions from the VP3/4A/4B assembly and VP4B/4C assembly

Fractions from VP3/4A/4B and VP4B/4C were analysed with mouse antiserum prepared against whole Nora virus (1:500). As a secondary antibody, goat anti-mouse IgG Fc conjugated with alkaline phosphatase was used. **(a)** Lane 1: Spectra broad range protein ladder, Lane 2: recombinant virus control (mixture of all cloned Nora virus proteins), Lanes 3–12: VP3/4A/4B assembly fractions. Red box indicates the fraction containing desired protein sizes at ~32 kDa (VP4B), ~35 kDa (VP3) and ~37 kDa (VP4A). **(b)** Lane 1: Spectra broad range protein ladder, Lane 2: recombinant virus control (mixture of all cloned Nora virus proteins), Lanes 3–12: VP4B/4C assembly fractions. Red box indicates the fractions containing desired protein sizes at ~32 kDa (VP4B) and ~49 kDa (VP4C).

ferred to as the upper band and the lower band. The lower band was denser since it contained the Nora virus genomic RNA and it was smaller in diameter than the upper band (Ericson *et al.*, 2016). This has been shown with other viruses as completed virions became denser as the genetic material condensed and the protein shell compressed around the genome (Black, 1989; Roos *et al.*, 2007). For this study, the upper band is more important to compare to our VLPs since it represents empty capsids and our VLPs would not have any viral RNA to package in the assembly. The upper band particles had diameters measured from EM images and twenty-two measured particles were used for a comparison to the different assembly groups. For the statistical test, 63 measured particles were used for VP3/4A/4B/4C, 20 for VP3/4B/4C, 27 for VP3/4A/4B, 59 for VP4A/4B/4C, 11 for VP3/4A, 24 for VP3/4B, 40 for VP3/4C, 28 for VP4A/4C, 22 for VP4B/4C, and 23 for VP4A.

Table 1. Average VLPs diameters measured from EM images of the various assemblies

Assembly	Average diameter (in nm)
VP3/4A/4B/4C	36.4 ± 2.94
VP3/4B/4C	92.8 ± 19.13
VP3/4A/4B	22.1 ± 0.95
VP4A/4B/4C	25.0 ± 1.17
VP3/4A	29.3 ± 2.47
VP3/4B	31.8 ± 2.84
VP3/4C	21.4 ± 1.02
VP4A/4C	22.9 ± 0.90
VP4B/4C	61.3 ± 18.56
VP4A	141.1 ± 24.28

(a)

(b)
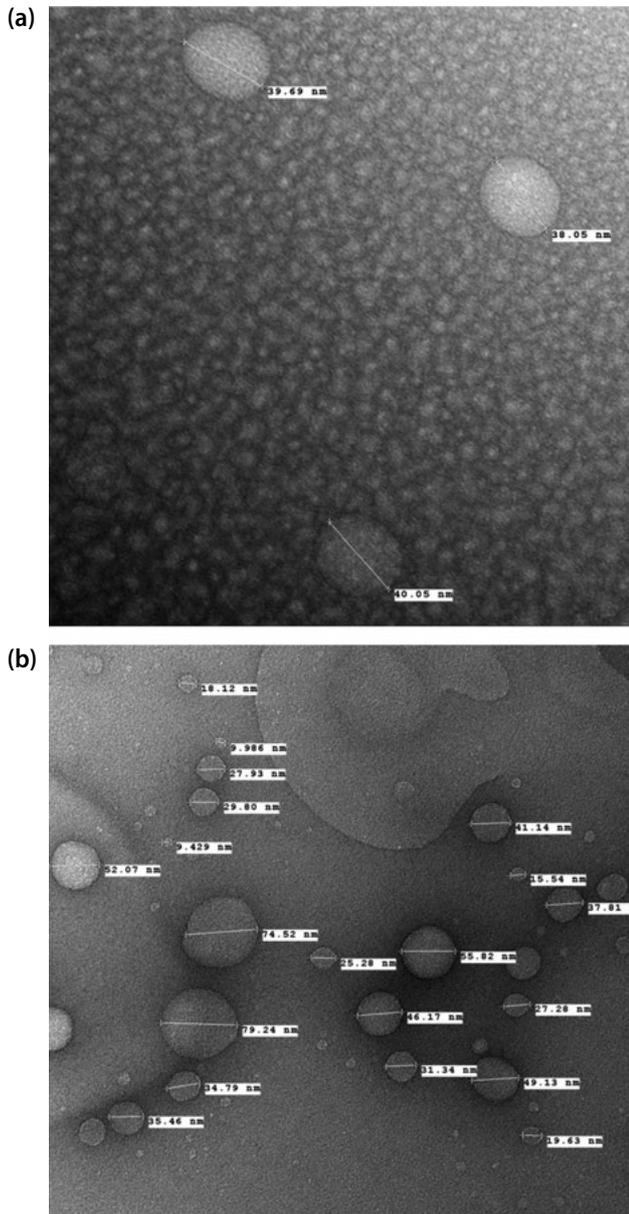
Fig. 2

EMs of representative VLP assembly fractions
(a) EM analysis of a single field of view of VP3/4A VLP assembly (350,000 x). **(b)** EM analysis of a single field of view of VP3/4A/4B/4C VLP assembly (150,000 x).

(a)

(b)

(c)

Fig. 3

Size distribution of Nora virus upper band empty capsids (control) and selected protein combinations of VLPs measured by EM

(a) From a CsCl gradient purification of whole Nora virus from *D. melanogaster*, two bands were represented (Ericson *et al.*, 2016). The lower band represents complete Nora virus virions while the upper band represents empty capsids. Diameters of the empty capsids were randomly measured from the EM images. Size distribution of upper band particles were between 21 and 30 nm, with several larger particles within 31 to 40 nm in size (average diameter = 30.4 ± 0.43 nm, n = 22). **(b)** Size distribution of VP3/4A VLPs were between 17 and 40 nm (average diameter = 29.3 ± 2.47 nm, n = 11). **(c)** Size distribution of VP3/4A/4B/4C VLPs were between 9 and 84 nm, with 20% of the particles larger than 50 nm (average diameter = 36.4 ± 2.94 nm, n = 61).

were similar to empty capsid of Nora virus. The upper band empty capsids averaged 30.4 nm in diameter. One of the fifty-nine VP4A/4B/4C and two of the sixty-two VP3/4A/4B/4C VLPs were removed as outliers as assessed by the Grubbs test (2.2 standard deviations) (Grubbs, 1969; Burns *et al.*, 2005). Statistical analysis using a one-way ANOVA between upper band or VP4A assembly compared to the different assembled protein combinations were

Fig. 4

Data analysis from EM diameter measurements of VLPs assemblies

Different protein combination VLPs assemblies are designated on the X-axis and average diameters of VLPs, in nanometers, is given on the Y-axis. VP4A, VP4B/4C, and VP3/4B/4C were significantly different from the upper band (* = p ≤0.05). All assemblies were significantly different from VP4A (p ≤0.0007). Error bars are standard error of the mean.

found to be significant (p = 1.14 x 10^{-13} and p = 1.11 x 10^{-16}, respectively). Holm-Bonferroni post-hoc tests comparing the upper band to all assemblies showed three protein combination groups being significantly different (Fig. 4). The three significantly different protein groups are VP4A, VP4B/4C, and VP3/4B/4C (p = 5.88 x 10^{-5}, 0.020416, and 4.90 x 10^{-8}, respectively). When doing the same type of analysis and comparing all assemblies to VP4A, all assemblies were significantly different (p ≤0.0007, Fig. 4).

Discussion

Viruses in the family *Picornaviridae* are structurally very simple, containing only single stranded plus-sense RNA surrounded by an icosahedral protein capsid. In the life cycle of picornaviruses, like poliovirus and bovine enterovirus, structural proteins are translated, undergo cleavage, and then start to assemble. Various structural proteins will associate to form a protomer and five protomers arrange into one pentamer. Twelve pentamers subsequently assemble to form a procapsid, which fills with RNA to construct a provirion (Basavappa *et al.*, 1994; Li *et al.*, 2012). Since a mature virion only has proteins and RNA, the assembly must involve only two types of interactions: capsid protein-capsid protein and capsid protein-RNA attractions (Garmann *et al.*, 2014; Buzón *et al.*, 2020). Under the right conditions, viral capsids have been shown to assemble spontaneously and form VLPs

due to capsid protein-capsid protein interactions (Nguyen and Brooks, 2008; Garmann *et al.*, 2014; Bajaj and Banerjee, 2016). In this study, different combinations of Nora virus structural proteins were mixed *in vitro* to assemble VLPs and study the role of the proteins in viral structure and/ or stability.

After fractionating an assembly reaction, the first step in VLPs detection was running a Western blot to verify positive fractions. Positive fractions for Nora virus proteins were viewed via EM and random VLPs were measured. Of the ten different combinations of proteins dialyzed, fractionated, and examined via EM, all showed some assembly. Among the assemblies, some showed a narrow range in the diameter sizes of VLPs while other assemblies resulted in a broad distribution of VLPs varying in size from small to large particles. *In vivo*, the spontaneous self-assembly of capsid proteins into symmetric capsids results in high physical homogeneity and rarely results in unusual particles. However, assembly under non-native conditions, like *in vitro*, can have capsid proteins readily forming VLPs with "alternative forms" (Nguyen and Brooks, 2008; Bajaj and Banerjee, 2016). *In vitro* studies resulting in VLPs with different morphology (from those assembled *in vivo*), were due to mutated capsid proteins, changes in assembly pH, availability of cations in assembly, and changes in ionic strength (Salunke *et al.*, 1989; Sastri *et al.*, 1997; Kanesashi *et al.*, 2003; Bajaj and Banerjee, 2016). These different VLP forms generally are the result of small partial assemblies and large ag-

gregated particles. All of our assemblies have at least one VLP that was smaller (< 20 nm diameter) than expected, which could be explained as a partial assembly of viral particles (Nguyen and Brooks, 2008). Several assemblies have at least one particle that was larger (> 40 nm) than expected, which could be a result of protein aggregation (Zeltins, 2012). Protein aggregations can be an issue in VLP production. Ding *et al.* (2010) performed a modeling study and showed that unproductive aggregations compete with the self-assembling subunits, therefore, limiting capsid growth. Therefore, in assemblies containing large amounts of aggregations, there could have been a limiting factor affecting normal VLP construction and growth. For a few viruses, like minute virus of mice and hepatitis B virus, it is normal during viral assembly for the production of large incomplete capsids in addition to small capsid intermediates. Since these are DNA viruses, it is highly unlikely that Nora virus assembly is following this model of capsid production. These partial assemblies and aggregates were also found in an *in vitro* assembly study involving flock house virus. This virus is similar to Nora virus in size, has an RNA genome, and infects insects. The expression of the single flock house virus structural protein was done in *E. coli,* followed by *in vitro* assembly, leading to a heterogeneous population of particles (Bajaj and Banerjee, 2016). Even though we see the same variation in VLPs in our *in vitro* study, we cannot ignore that Nora virus involves several proteins interacting to form the capsid, not one protein as in flock house virus. Also, a computer simulation study looked at the probability of T=1 and T=3 icosahedral capsid formations in assembly reactions. Altering a few variables from the native virus environment of assembly (a high protein concentration or low temperature) led to capsids with skewed or alternate forms. Some particles known as "monster particles" were shown from the models and had diverse morphology (Nguyen and Brooks, 2008). If our conditions were not ideal for VLP formation, this could explain the diversity and the larger particles seen in some assemblies. Perhaps the environment for our *in vitro* assemblies has variables different from the *D. melanogaster in vivo* environment or is missing specific control proteins from the host cell resulting in the presence of the misassembled capsids.

In an attempt to discern which Nora virus protein is important in capsid formation or virus assembly, statistical analysis of VLP diameter sizes compared to the upper band were performed. Three assemblies, VP4B/4C, VP3/4B/4C, and VP4A alone are statistically different from the upper band. The average diameter of the VP4A assembly alone was very large with several particles >50 nm. This could be a result of VP4A dimerizing, causing large aggregated particles (Zeltins, 2012). It was not expected that using only one capsid protein would result in VLP

formation. All other assemblies that were statistically similar to the upper band had either VP4A or VP3 present. An exception was the VP3/4B/4C assembly, which became statistically similar once VP4A was added back (assembly VP3/4A/4B/4C). This suggests VP3 may be needed for assembly but in our study, it seems as though VP4A is more important in VLP formation and/or stability. All VLP assemblies containing VP4A were not statistically different from incomplete empty capsids. A recent study showed a Nora virus reconstruction that displayed the virus as being an icosahedrally symmetric particle with a T=1 (pseudo T=3) triangulation number. Intra-pentamer stability of the capsid results from the interaction of VP4B and VP4C while inter-pentamer stability is displayed by VP4A proteins that additionally interact with the viral RNA. This inter-pentamer stability is due to a crossover of the VP4A N-terminus with the N-terminus of another VP4A in a neighboring pentamer (Laurinmäki *et al.*, 2020). A past study demonstrated the importance of VP3 in the stability and for the horizontal transmission of Nora viruses. When the coiled-coil domain of VP3 was disrupted, these characteristics were lost (Sadanandan *et al.,* 2016). But the recent Laurinmäki study suggests that VP3 is not required for capsid assembly but does still maintain a role in stability (Laurinmäki *et al.*, 2020). Our results show that VP3 may be playing a minor role in assembly while still involved in stability of the capsid. Due to our results, we postulate that VP4A must be present with other proteins (VP4B and/or VP4C) to begin capsid assembly and provide inter-pentamer stability. In addition, our data suggests that VP3 has a minor role in assembly and/or stability, but without VP4A, in most cases, the capsid will not form at the correct size. Currently, we cannot discern the order of assembly of the proteins to create the capsid, but it is a question to be further investigated.

In summary, the data indicate that there was successful assembly of Nora virus VLPs via an *in vitro* method using purified proteins under controlled conditions. Some assemblies had little variation is VLP size, while others had a heterogeneous population of particles. These *in vitro* methodologies of assembly were important in the past to determine virus structure and assembly while also being applied for vaccine development and more recently for virus-based nanostructures in nanomedicine and nanotechnology (Bajaj and Banerjee, 2016). Our data does show that VP3 may be important and playing a minor role in VLP formation or is important in the stability of newly formed particles. Overall, the study revealed VLP sizes statistically similar to that of empty capsid virus when the assembly contained VP4A with an additional protein. This supports the aim that VP4A may be a major protein for capsid assembly and/or stability. Future directions may include changes to assembly conditions, alterations

to the capsid proteins used in assembly, providing viral RNA to encourage the production of complete virions, or the development of a cell culture system to propagate VLPs. Overall, determining the role of VP3, VP4A, VP4B, and VP4C in capsid assembly and the pathway to this assembly is important in determining how the virus forms and replicates not only for Nora viruses, but also other picornaviruses.

References

Aickin M, Gensler H (1996): Adjusting for multiple testing when reporting research results: the Bonferroni vs Holm methods. Am. J. Public Health 86(5), 726–728. https://doi.org/10.2105/AJPH.86.5.726

Bajaj S, Banerjee M (2016): In vitro assembly of polymorphic virus-like particles from the capsid protein of a nodavirus. Virology 496, 106–115. https://doi.org/10.1016/j.virol.2016.05.025

Bancroft J, Hiebert E (1967): Formation of an infectious nucleoprotein from protein and nucleic acid isolated from a small spherical virus. Virology 32, 354–356. https://doi.org/10.1016/0042-6822(67)90284-X

Basavappa R, Syed R, Flore O, Icenogle JP, Filman DJ, Hogle JM (1994): Role and mechanism of the maturation cleavage of VP0 in poliovirus assembly: structure of the empty capsid assembly intermediate at 2.0 Å resolution. Protein Sci. 3(10), 1651–1669. https://doi.org/10.1002/pro.5560031005

Black LW (1989): DNA packaging in dsDNA bacteriophages. Annu. Rev. Microbiol. 43, 267–292. https://doi.org/10.1146/annurev.mi.43.100189.001411

Bräutigam S, Snezhkov E, Bishop DHL (1993): Formation of poliovirus-like particles by recombinant baculoviruses expressing the individual VP0, VP3, and VP1 proteins by comparison to particles derived from the expressed poliovirus polyprotein. Virology 192(2), 512–524. https://doi.org/10.1006/viro.1993.1067

Burns MJ, Nixon GJ, Foy CA, Harris N (2005): Standardisation of data from real-time quantitative PCR methods - evaluation of outliers and comparison of calibration curves. BMC Biotechnol. 5(31), 1–13. https://doi.org/10.1186/1472-6750-5-31

Buzón P, Maity S, Roos WH (2020): Physical virology: from virus self-assembly to particle mechanics. WIREs Nanomed. Nanobiotechnol. 12(4), e1613. https://doi.org/10.1002/wnan.1613

Carreira A, Menendez M, Reguera J, Almendral JM, Mateu MG (2004): In vitro disassembly of a parvovirus capsid and effect on capsid stability of heterologous peptide insertions in surface loops. J. Biol. Chem. 279(8), 6517–6525. https://doi.org/10.1074/jbc.M307662200

Chung Y-C, Ho M-S, Wu J-C, Chen W-J, Huang J-H, Chou S-T, Hu Y-C (2008): Immunization with virus-like particles of enterovirus 71 elicits potent immune responses and protects mice against lethal challenge. Vaccine 26(15), 1855–1862. https://doi.org/10.1016/j.vaccine.2008.01.058

Crawford SE, Labbé M, Cohen J, Burroughs MH, Zhou Y-J, Estes MK (1994): Characterization of virus-like particles produced by the expression of rotavirus capsid proteins in insect cells. J. Virol. 68(9), 5945–5952. https://doi.org/10.1128/jvi.68.9.5945-5952.1994

Ding Y, Chuan YP, He L, Middelberg APJ (2010): Modeling the competition between aggregation and self-assembly during virus-like particle processing. Biotechnol. Bioeng. 107(3), 550–560. https://doi.org/10.1002/bit.22821

Ekström J-O, Habayeb MS, Srivastava V, Kieselbach T, Wingsle G, Hultmark D (2011): Drosophila Nora virus capsid proteins differ from those of other picorna-like viruses. Virus Res. 160(1–2), 51–58. https://doi.org/10.1016/j.virusres.2011.05.006

Ericson BL, Carlson DJ, Carlson KA (2016): Characterization of Nora virus structural proteins via Western blot analysis. Scientifica Article ID 9067848. https://doi.org/10.1155/2016/9067848. https://doi.org/10.1155/2016/9067848

Fraenkel-Conrat H, Williams RC (1955): Reconstitution of active tobacco mosaic virus from its inactive protein and nucleic acid components. PNAS 41, 690–698. https://doi.org/10.1073/pnas.41.10.690

Garmann RF, Comas-Garcia M, Gopal A, Knobler CM, Gelbart WM (2014): The assembly pathway of an icosahedral single-stranded RNA virus depends on the strength of inter-subunit attractions. J. Mol. Biol. 426(5), 1050–1060. https://doi.org/10.1016/j.jmb.2013.10.017

Grgacic EVL, Anderson DA (2006): Virus-like particles: passport to immune recognition. Methods 40(1), 60–65. https://doi.org/10.1016/j.ymeth.2006.07.018

Grubbs FE (1969): Procedure for detecting outlying observations in samples. Technometrics 11(1), 1–21. https://doi.org/10.1080/00401706.1969.10490657

Habayeb MS, Ekengren SK, Hultmark D (2006): Nora virus, a persistent virus in Drosophila, defines a new picorna-like

virus family. J. Gen. Virol. 87(10), 3045–3051. https://doi.org/10.1099/vir.0.81997-0

Habayeb MS, Cantera R, Casanova G, Ekström J-O, Albright S, Hultmark D (2009a): The Drosophila Nora virus is an enteric virus, transmitted via feces. J. Invertebr. Pathol. 101(1), 29–33. https://doi.org/10.1016/j.jip.2009.02.003

Habayeb MS, Ekström J-O, Hultmark D (2009b): Nora virus persistent infections are not affected by RNAi machinery. PLoS One 4, 1–5. https://doi.org/10.1371/journal.pone.0005731

Kanesashi S-N, Ishizu K-I, Kawano M-A, Han S-I, Tomita S, Watanabe H, Kataoka K, Handa H (2003): Simian virus 40 VP1 capsid protein forms polymorphic assemblies in vitro. J. Gen. Virol. 84(7), 1899–1905. https://doi.org/10.1099/vir.0.19067-0

Klingel K, Hohenadl C, Canu A, Albrecht M, Seemann M, Mall G, Kandolf R (1992): Ongoing enterovirus-induced myocarditis is associated with persistent heart muscle infection: quantitative analysis of virus replication, tissue damage, and inflammation. PNAS 89(1), 314–318. https://doi.org/10.1073/pnas.89.1.314

Koonin EV, Wolf YI, Nagasaki K, Dolja VV (2008): The big bang of picorna-like virus evolution antedates the radiation of eukaryotic supergroups. Nat. Rev. Microbiol. 6, 925–939. https://doi.org/10.1038/nrmicro2030

Koutsky LA, Ault KA, Wheeler CM, Brown DR, Barr E, Alvarz FB, Chiacchierini LM, Jansen KU (2002): A controlled trial of a human papillomavirus type 16 vaccine. N. Engl. J. Med. 347(21), 1645–1651. https://doi.org/10.1056/NEJMoa020586

Laurinmäki P, Shakell S, Ekström J-O, Mohammadi P, Hultmark D, Butcher SJ (2020) Structure of Nora virus at 2.7 Å resolution and implications for receptor binding, capsid stability and taxonomy. Sci. Rep. 10(19675). https://doi.org/10.1038/s41598-020-76613-1

Li C, Wang JC-Y, Taylor MW, Zlotnick A (2012): In vitro assembly of an empty picornavirus capsid follows a dodecahedral path. J. Virol. 86(23), 13062–13069. https://doi.org/10.1128/JVI.01033-12

Mohsen MO, Zha L, Cabral-Miranda G, Bachmann MF (2017): Major findings and recent advances in virus-like particle (VLP)-based vaccines. Semin. Immunol. 34, 123–132. https://doi.org/10.1016/j.smim.2017.08.014

Nguyen HD, Brooks III CL (2008): Generalized structural polymorphism in self-assembled viral particles. Nano Letters 8, 4574–4581. https://doi.org/10.1021/nl802828v

Noad R, Roy P (2003): Virus-like particles as immunogens. Trends Microbiol. 11(9), 438–444. https://doi.org/10.1016/S0966-842X(03)00208-7

Pattenden LK, Middelberg APJ, Niebert M, Lipin DI (2005): Towards the preparative and large-scale precision manufacture of virus-like particles. Trends

Biotechnol. 23(10), 523–529. https://doi.org/10.1016/j.tibtech.2005.07.011

Rogers A, Towery L, McCown A, Carlson KA (2020): Impaired geotaxis as a novel phenotype of Nora virus infection of Drosophila melanogaster. Scientifica Article ID 1804510. https://doi.org/10.1155/2020/1804510

Roos WH, Ivanovska IL, Evilevitch A, Wuite GJL (2007): Viral capsids: mechanical characteristics, genome packaging and delivery mechanisms. Cell. Mol. Life Sci. 64, 1484–1497. https://doi.org/10.1007/s00018-007-6451-1

Rueckert RR (1996): Picornaviridae: The viruses and their replication. In Fields BN, Knipe DM, Howley PM, Chanock RM, Melnick JL, Monath TP, Rotzman B, Straus SE, (Eds): Field's Virology. Vol 1, 3rd Ed. Lippincott-Raven: USA, pp. 609–654.

Sadanandan SA, Ekström J-O, Jonna VR, Hofer A, Hultmark D (2016): VP3 is crucial for the stability of Nora virus virions. Virus Res. 223, 20–27. https://doi.org/10.1016/j.virusres.2016.06.011

Salunke DM, Caspar DL, Garcea RL (1989): Polymorphism in the assembly of polyomavirus capsid protein VP1. Biophys. J. 56(5), 887–900. https://doi.org/10.1016/S0006-3495(89)82735-3

Sanchez-Rodriguez SP, Munch-Anguiano L, Echeverria O, Vazquez-Nin G, Mora-Pale M, Dordick JS, Bustos-Jaimes I (2012): Human parvovirus B19 virus-like particles: in vitro assembly and stability. Biochimie 94(3), 870–878. https://doi.org/10.1016/j.biochi.2011.12.006

Sanfaçon H (2011): Biodiversity and evolution of picorna-like viruses. Biodivers. 7(1), 45–50. https://doi.org/10.1080/14888386.2006.9712794

Sastri M, Kekuda R, Gopinath K, Ranjith Kumar CT, Jagath JR, Savithri HS (1997): Assembly of physalis mottle virus capsid protein in Escherichia coli and the role of amino and carboxy termini in the formation of the icosahedral particles. J. Mol. Biol. 272(4), 541–552. https://doi.org/10.1006/jmbi.1997.1258

van Mierlo JT, Bronkhorst AW, Overheul GJ, Sadanandan SA, Ekström J-O, Heestermans M, Hultmark D, Antoniewski C, van Rij RP (2012): Convergent evolution of argonaute-2 slicer antagonism in two distinct insect RNA viruses. PLoS Pathog. 8(8), e1002872. https://doi.org/10.1371/journal.ppat.1002872

Zeltins A (2012): Construction and characterization of virus-like particles: a review. Mol. Biotechnol. 53(1), 92–107. https://doi.org/10.1007/s12033-012-9598-4

Zhang L, Parham NJ, Zhang F, Aasa-Chapman M, Gould EA, Zhang H (2012): Vaccination with coxsackievirus B3 virus-like particles elicits humoral immune response and protects mice against myocarditis. Vaccine 30(13), 2301–2308. https://doi.org/10.1016/j.vaccine.2012.01.061